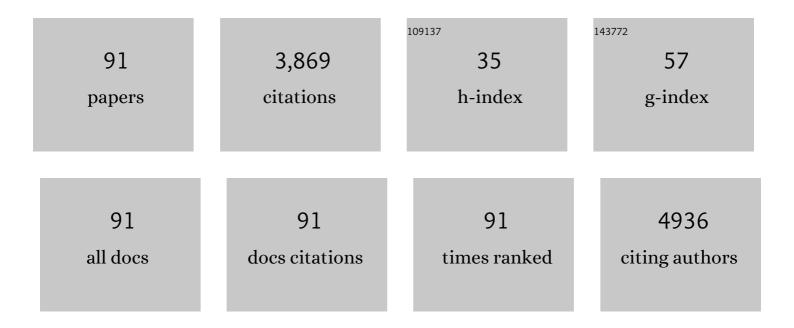
List of Publications by Year in descending order

Source: https://exaly.com/author-pdf/916779/publications.pdf Version: 2024-02-01



DONC SHU

#	Article	IF	CITATIONS
1	Realizing a redox-robust Ag/MnO2 catalyst for efficient wet catalytic ozonation of S-VOCs: Promotional role of Ag(0)/Ag(I)-Mn based redox shuttle. Applied Catalysis B: Environmental, 2022, 303, 120881.	10.8	43
2	Hollow NiCoP nanocubes derived from a Prussian blue analogue self-template for high-performance supercapacitors. Journal of Alloys and Compounds, 2022, 893, 162344.	2.8	37
3	Electron-rich/poor reaction sites enable ultrafast confining Fenton-like processes in facet-engineered BiOI membranes for water purification. Applied Catalysis B: Environmental, 2022, 304, 120970.	10.8	34
4	Molecular cooking: Amino acids trap silicon in carbon matrix to boost lithium-ion storage. Energy Storage Materials, 2022, 46, 344-351.	9.5	25
5	Boosting the energy density of supercapacitors by designing both hollow NiO nanoparticles/nitrogen-doped carbon cathode and nitrogen-doped carbon anode from the same precursor. Chemical Engineering Journal, 2022, 431, 134083.	6.6	62
6	Metal organic frameworks derived Ni-doped hierarchical NiXCo1-XS@C bundled-like nanostructures for enhanced supercapacitors. Electrochimica Acta, 2022, 406, 139872.	2.6	23
7	Design of few-layered 1T-MoS2 by supramolecular-assisted assembly with N-doped carbon quantum dots for supercapacitor. Journal of Electroanalytical Chemistry, 2022, 908, 116093.	1.9	17
8	Dual-Functional Tungsten Boosted Lithium-Ion Diffusion and Structural Integrity of LiNi _{0.8} Co _{0.1} Mn _{0.1} O ₂ Cathodes for High Performance Lithium-Ion Batteries. ACS Sustainable Chemistry and Engineering, 2022, 10, 50-60.	3.2	7
9	Graphene Quantum Dots Pinned on Nanosheetsâ€Assembled NiCoâ€LDH Hollow Microâ€Tunnels: Toward Highâ€Performance Pouchâ€Type Supercapacitor via the Regulated Electron Localization. Small, 2022, 18, e2201286.	5.2	48
10	Efficient catalytic activity and bromate minimization over lattice oxygen-rich MnOOH nanorods in catalytic ozonation of bromide-containing organic pollutants: Lattice oxygen-directed redox cycle and bromate reduction. Journal of Hazardous Materials, 2021, 410, 124545.	6.5	27
11	Defect-Engineered 3D Cross-Network Co ₃ O _{4–<i>x</i>} N _{<i>x</i>} Nanostructure for High-Performance Solid-State Asymmetric Supercapacitors. ACS Applied Energy Materials, 2021, 4, 888-898.	2.5	15
12	Supramolecular assisted fabrication of Mn3O4 anchored nitrogen-doped reduced graphene oxide and its distinctive electrochemical activation process during supercapacitive study. Electrochimica Acta, 2021, 370, 137739.	2.6	15
13	Enhanced structural and electrochemical stability of LiNi0.83Co0.11Mn0.06O2 cathodes by zirconium and aluminum co-doping for lithium-ion battery. Journal of Power Sources, 2021, 498, 229857.	4.0	19
14	Nest-like N-doped hierarchical porous active carbon formed by sacrifice template for enhanced supercapacitor. Ionics, 2021, 27, 4461-4471.	1.2	4
15	Multifunctional Au/Ti ₃ C ₂ Photothermal Membrane with Antibacterial Ability for Stable and Efficient Solar Water Purification under the Full Spectrum. ACS Sustainable Chemistry and Engineering, 2021, 9, 11372-11387.	3.2	40
16	Metal organic framework derived hollow NiS@C with S-vacancies to boost high-performance supercapacitors. Chemical Engineering Journal, 2021, 419, 129643.	6.6	77
17	Promoting high-energy supercapacitor performance over NiCoP/N-doped carbon hybrid hollow nanocages via rational architectural and electronic modulation. Applied Surface Science, 2021, 569, 151098.	3.1	31
18	Urchin-like NiCo ₂ O ₄ hollow microspheres with oxygen vacancies synthesized by self-template for supercapacitor. New Journal of Chemistry, 2021, 45, 22748-22757.	1.4	22

#	Article	IF	CITATIONS
19	Activation of persulfate by CuO-sludge-derived carbon dispersed on silicon carbide foams for odorous methyl mercaptan elimination: identification of reactive oxygen species. Environmental Science and Pollution Research, 2020, 27, 1224-1233.	2.7	12
20	In-situ fabrication of AgI-BiOI nanoflake arrays film photoelectrode for efficient wastewater treatment, electricity production and enhanced recovery of copper in photocatalytic fuel cell. Catalysis Today, 2020, 339, 379-390.	2.2	20
21	Engineered photocatalytic fuel cell with oxygen vacancies-rich rGO/BiO1â^²xI as photoanode and biomass-derived N-doped carbon as cathode: Promotion of reactive oxygen species production via Fe2+/Fe3+ redox. Chemical Engineering Journal, 2020, 385, 123824.	6.6	43
22	Interfacial electrostatic self-assembly in water-in-oil microemulsion assisted synthesis of Li4Ti5O12/Graphene for lithium-ion-batteries. Journal of Alloys and Compounds, 2020, 819, 153018.	2.8	18
23	Hollow N-doped carbon @ O-vacancies NiCo2O4 nanocages with a built-in electric field as high-performance cathodes for hybrid supercapacitor. Electrochimica Acta, 2020, 364, 137260.	2.6	42
24	Supramolecular-induced confining methylene blue in three-dimensional reduced graphene oxide for high-performance supercapacitors. Journal of Power Sources, 2020, 475, 228554.	4.0	34
25	Preparation of Single-Atom Ag-Decorated MnO ₂ Hollow Microspheres by Redox Etching Method for High-Performance Solid-State Asymmetric Supercapacitors. ACS Applied Energy Materials, 2020, 3, 10192-10201.	2.5	22
26	Mechanism of a Lithiated Interlayer for Improving the Cycle Life of High Voltage Li-Ion Batteries Using a Commercial Carbonate Electrolyte. Journal of Physical Chemistry C, 2020, 124, 8057-8066.	1.5	5
27	Holey graphene/MnO ₂ nanosheets with open ion channels for highâ€performance solidâ€state asymmetric supercapacitors. International Journal of Energy Research, 2020, 44, 3446-3457.	2.2	10
28	Layered molybdenum disulfide coated carbon hollow spheres synthesized through supramolecular selfâ€assembly applied to supercapacitors. International Journal of Energy Research, 2020, 44, 7082-7092.	2.2	14
29	Investigation on the pseudocapacitive charge storage mechanism of MnO2 in various electrolytes by electrochemical quartz crystal microbalance (EQCM). Ionics, 2019, 25, 2393-2399.	1.2	4
30	In-situ N/S Co-doping three-dimensional succulent-like hierarchical carbon assisted by supramolecular polymerization for high-performance supercapacitors. Electrochimica Acta, 2019, 319, 410-422.	2.6	40
31	Anchoring ultrafine Co3O4 grains on reduced oxide graphene by dual-template nanocasting strategy for high-energy solid state supercapacitor. Electrochimica Acta, 2019, 326, 134965.	2.6	35
32	Immobilization of facet-engineered Ag3PO4 on mesoporous Al2O3 for efficient industrial waste gas purification with indoor LED illumination. Applied Catalysis B: Environmental, 2019, 256, 117811.	10.8	27
33	Supermolecule Self-Assembly Promoted Porous N, P Co-Doped Reduced Graphene Oxide for High Energy Density Supercapacitors. ACS Applied Energy Materials, 2019, 2, 4084-4091.	2.5	45
34	Mycelial pellet-derived heteroatom-doped carbon nanosheets with a three-dimensional hierarchical porous structure for efficient capacitive deionization. Environmental Science: Nano, 2019, 6, 1430-1442.	2.2	33
35	High-performance water desalination of heteroatom nitrogen- and sulfur-codoped open hollow tubular porous carbon electrodes <i>via</i> capacitive deionization. Environmental Science: Nano, 2019, 6, 3359-3373.	2.2	31
36	Synthesis of three dimensional N&S co-doped rGO foam with high capacity and long cycling stability for supercapacitors. Journal of Colloid and Interface Science, 2019, 537, 57-65.	5.0	29

#	Article	IF	CITATIONS
37	3D sandwiched nanosheet of MoS2/C@RGO achieved by supramolecular self-assembly method as high performance material in supercapacitor. Journal of Alloys and Compounds, 2019, 777, 1176-1183.	2.8	38
38	Analysis on the constant-current overcharge electrode process and self-protection mechanism of LiCoO2/graphite batteries. Journal of Solid State Electrochemistry, 2019, 23, 407-417.	1.2	5
39	Supramolecule-assisted synthesis of in-situ carbon-coated MnO2 nanosphere for supercapacitors. Journal of Alloys and Compounds, 2019, 779, 550-556.	2.8	13
40	In Situ Supramolecular Self-Assembly Assisted Synthesis of Li ₄ Ti ₅ O ₁₂ –Carbon-Reduced Graphene Oxide Microspheres for Lithium-Ion Batteries. ACS Sustainable Chemistry and Engineering, 2019, 7, 916-924.	3.2	23
41	Molecular self-assembly assisted synthesis of carbon nanoparticle-anchored MoS2 nanosheets for high-performance supercapacitors. Electrochimica Acta, 2019, 295, 187-194.	2.6	27
42	Preparation of carbon dots decorated graphene/polyaniline composites by supramolecular in-situ self-assembly for high-performance supercapacitors. Electrochimica Acta, 2019, 297, 1094-1103.	2.6	26
43	Chitosan-Confined Synthesis of N-Doped and Carbon-Coated Li ₄ Ti ₅ O ₁₂ Nanoparticles with Enhanced Lithium Storage for Lithium-Ion Batteries. Journal of the Electrochemical Society, 2018, 165, A1046-A1053.	1.3	32
44	Bio-templated fabrication of three-dimensional network activated carbons derived from mycelium pellets for supercapacitor applications. Scientific Reports, 2018, 8, 562.	1.6	24
45	One-step synthesis of silicon carbide foams supported hierarchical porous sludge-derived activated carbon as efficient odor gas adsorbent. Journal of Hazardous Materials, 2018, 344, 33-41.	6.5	28
46	3D MnO2 hollow microspheres ozone-catalysis coupled with flat-plate membrane filtration for continuous removal of organic pollutants: Efficient heterogeneous catalytic system and membrane fouling control. Journal of Hazardous Materials, 2018, 344, 1198-1208.	6.5	33
47	Surface modification of micro-sized CuO by in situ-growing heterojunctions CuO/Cu2O and CuO/Cu2O/Cu: effect on surface charges and photogenerated carrier lifetime. Applied Physics A: Materials Science and Processing, 2018, 124, 1.	1.1	16
48	Enhanced Performance and Conversion Pathway for Catalytic Ozonation of Methyl Mercaptan on Single-Atom Ag Deposited Three-Dimensional Ordered Mesoporous MnO ₂ . Environmental Science & Technology, 2018, 52, 13399-13409.	4.6	134
49	Carbohydrates-Derived Nitrogen-Doped Hierarchical Porous Carbon for Ultrasensitive Detection of 4-Nitrophenol. ACS Sustainable Chemistry and Engineering, 2018, 6, 17391-17401.	3.2	55
50	Supermolecule polymerization derived porous nitrogen-doped reduced graphene oxide as a high-performance electrode material for supercapacitors. Electrochimica Acta, 2018, 292, 20-30.	2.6	36
51	Three-dimensional hierarchical porous sludge-derived carbon supported on silicon carbide foams as effective and stable Fenton-like catalyst for odorous methyl mercaptan elimination. Journal of Hazardous Materials, 2018, 358, 136-144.	6.5	38
52	Highly Efficient Performance and Conversion Pathway of Photocatalytic CH ₃ SH Oxidation on Self-Stabilized Indirect Z-Scheme g-C ₃ N ₄ /I ^{3–} -BiOI. ACS Applied Materials & Interfaces, 2018, 10, 18693-18708.	4.0	75
53	Reaction Mechanisms of Sodiumâ€lon Batteries under Various Charge and Discharge Conditions in a Threeâ€Electrode Setup. ChemElectroChem, 2018, 5, 2475-2481.	1.7	4
54	Preparation of 3D Reduced Graphene Oxide/MnO ₂ Nanocomposites through a Vacuumâ€Impregnation Method and Their Electrochemical Capacitive Behavior. ChemElectroChem, 2017, 4, 1088-1094.	1.7	27

#	Article	IF	CITATIONS
55	Quinone Electrode Materials for Rechargeable Lithium/Sodium Ion Batteries. Advanced Energy Materials, 2017, 7, 1700278.	10.2	268
56	Combined adsorption and catalytic ozonation for removal of endocrine disrupting compounds over MWCNTs/Fe 3 O 4 composites. Catalysis Today, 2017, 297, 143-150.	2.2	37
57	MnO 2 -introduced-tunnels strategy for the preparation of nanotunnel inserted hierarchical-porous carbon as electrode material for high-performance supercapacitors. Chemical Engineering Journal, 2017, 320, 634-643.	6.6	33
58	Preparation of Lithium Titanate/Reduced Graphene Oxide Composites with Three-Dimensional "Fishnet-Like―Conductive Structure via a Gas-Foaming Method for High-Rate Lithium-Ion Batteries. ACS Applied Materials & Interfaces, 2017, 9, 42883-42892.	4.0	25
59	Elimination of methyl mercaptan in ZVI-S 2 O 8 2â^' system activated with in-situ generated ferrous ions from zero valent iron. Catalysis Today, 2017, 281, 520-526.	2.2	23
60	Three-dimensional MnO2 porous hollow microspheres for enhanced activity as ozonation catalysts in degradation of bisphenol A. Journal of Hazardous Materials, 2017, 321, 162-172.	6.5	175
61	Supramolecule-Inspired Fabrication of Carbon Nanoparticles In Situ Anchored Graphene Nanosheets Material for High-Performance Supercapacitors. ACS Applied Materials & Interfaces, 2016, 8, 26775-26782.	4.0	39
62	Heteroaromatic organic compound with conjugated multi-carbonyl as cathode material for rechargeable lithium batteries. Scientific Reports, 2016, 6, 23515.	1.6	34
63	Immobilization of self-stabilized plasmonic Ag-AgI on mesoporous Al2O3 for efficient purification of industrial waste gas with indoor LED illumination. Applied Catalysis B: Environmental, 2016, 185, 295-306.	10.8	26
64	Three-dimensional nitrogen-doped graphene hydrogels prepared via hydrothermal synthesis as high-performance supercapacitor materials. Electrochimica Acta, 2016, 194, 136-142.	2.6	107
65	Preparation of three-dimensional nitrogen-doped graphene layers by gas foaming method and its electrochemical capactive behavior. Electrochimica Acta, 2016, 193, 293-301.	2.6	15
66	Supercapacitive behavior of electrostatic self-assembly reduced graphene oxide/CoAl-layered double hydroxides nanocomposites. Journal of Alloys and Compounds, 2016, 669, 146-155.	2.8	50
67	Three-dimensional graphene layers prepared by a gas-foaming method for supercapacitor applications. Carbon, 2015, 94, 879-887.	5.4	107
68	Simultaneous photocatalytic elimination of gaseous NO and SO 2 in a BiOI/Al 2 O 3 -padded trickling scrubber under visible light. Chemical Engineering Journal, 2015, 279, 929-938.	6.6	50
69	Face-to-face self-assembly graphene/MnO2 nanocomposites for supercapacitor applications using electrochemically exfoliated graphene. Electrochimica Acta, 2015, 167, 412-420.	2.6	59
70	Effects of carbon additives on the performance of negative electrode of lead-carbon battery. Electrochimica Acta, 2015, 151, 89-98.	2.6	76
71	Recyclable CNTs/Fe3O4 magnetic nanocomposites as adsorbents to remove bisphenol A from water and their regeneration. Chemical Engineering Journal, 2015, 260, 231-239.	6.6	177
72	The supercapacitive behavior and excellent cycle stability of graphene/MnO 2 composite prepared by an electrostatic self-assembly process. International Journal of Hydrogen Energy, 2014, 39, 16151-16161.	3.8	36

#	Article	IF	CITATIONS
73	BiOI-based photoactivated fuel cell using refractory organic compounds as substrates to generate electricity. Catalysis Today, 2014, 224, 13-20.	2.2	40
74	Soft-template synthesis of vanadium oxynitride-carbon nanomaterials for supercapacitors. International Journal of Hydrogen Energy, 2014, 39, 16139-16150.	3.8	35
75	Preferential catalytic ozonation of p-nitrophenol by molecularly imprinted Fe3O4/SiO2 core-shell magnetic composites. Water Science and Technology, 2014, 69, 170-176.	1.2	15
76	Capacitive performance of a heteroatom-enriched activated carbon inÂconcentrated sulfuric acid. Journal of Power Sources, 2013, 239, 553-560.	4.0	20
77	pH-dependent degradation of acid orange II by zero-valent iron in presence of oxygen. Separation and Purification Technology, 2013, 117, 59-68.	3.9	69
78	Visible-light-harvesting reduction of CO2 to chemical fuels with plasmonic Ag@AgBr/CNT nanocomposites. Catalysis Today, 2013, 216, 268-275.	2.2	65
79	Disinfection of E. Coli Using Visible-light-driven Photocatalyst. Procedia Environmental Sciences, 2013, 18, 503-508.	1.3	8
80	Fabrication and supercapacitive behavior of tetramethylammonium ion-intercalated MnO2 prepared by an exfoliation and self-assembly process. Journal of Alloys and Compounds, 2013, 569, 136-143.	2.8	18
81	Lithium-Ion Batteries: Recent Advances and New Horizons. International Journal of Electrochemistry, 2012, 2012, 1-2.	2.4	2
82	Enhanced adsorption and photocatalytic activity of BiOl–MWCNT composites towards organic pollutants in aqueous solution. Journal of Hazardous Materials, 2012, 229-230, 72-82.	6.5	90
83	Capacitive properties of PANI/MnO2 synthesized via simultaneous-oxidation route. Journal of Alloys and Compounds, 2012, 532, 1-9.	2.8	84
84	Microstructure and supercapacitive properties of buserite-type manganese oxide with a large basal spacing. Journal of Power Sources, 2012, 216, 425-433.	4.0	27
85	Enhanced photocatalytic disinfection of E. coli 8099 using Ag/BiOI composite under visible light irradiation. Separation and Purification Technology, 2012, 91, 59-66.	3.9	97
86	Supercapacitive behavior and high cycle stability of todorokite-type manganese oxide with large tunnels. Journal of Power Sources, 2012, 203, 233-242.	4.0	46
87	Preparation of nanocrystalline VN by the melamine reduction of V2O5 xerogel and its supercapacitive behavior. Materials Chemistry and Physics, 2011, 131, 268-273.	2.0	77
88	Photocatalytic activity of metal (Pt, Ag, and Cu)-deposited TiO2 photoelectrodes for degradation of organic pollutants in aqueous solution. Desalination, 2010, 253, 88-93.	4.0	45
89	Preparation of novel layered AgBr-based inorganic/organic nanosheets by pulsed laser ablation in aqueous media. , 2010, , .		0
90	Study on the electrochemical behavior of vanadium nitride as a promising supercapacitor material. Journal of Physics and Chemistry of Solids, 2009, 70, 495-500.	1.9	142

#	Article	IF	CITATIONS
91	Improved electrochemical redox performance of 2,5-dimercapto-1,3,4-thiadiazole by poly(3-methoxythiophene). Journal of Applied Electrochemistry, 2006, 36, 1427-1431.	1.5	8